Wavelet Correlogram: A New Approach for Image Indexing and Retrieval

H. Abrishami Moghaddam[*1], T. Taghizadeh Khajoie[2], A.H. Rouhi[2], M. Saadatmand Tarzjan[1]

1. K.N. Toosi University of Technology

Seyed Khandan P.O. Box 16315-1355, Tehran, Iran

moghadam@saba.kntu.ac.ir
msaadat59@yahoo.com

2. AZAD University, Science & Research Unit

P.O. Box 19395-3755, Tehran, Iran

ttaghizadeh@noavar.com
ahrouhi@yahoo.com

[*] Corresponding Author

Corresponding Author

Hamid Abrishami Moghaddam (Ph.D.)

Electrical Engineering Department

K. N. Toosi University of Technology

Seyed Khandan

P.O. Box 16315-1355

Tehran, Iran

Tel: +98 21 8461025

Fax: +98 21 8462066

E-mail: moghadam@saba.kntu.ac.ir

Summary

Storage and retrieval of images in digital libraries become a real demand in industrial, medical, and other applications. Current image indexing and retrieval systems are based on two major approaches including spatial and transform domain-based methods. The first approach usually uses pixel (or a group of adjacent pixels) features like color and shape, while the second approach uses the data in transform domain such as wavelets. This paper presents a new algorithm for content-based image indexing and retrieval to be used in digital libraries. The proposed method is based on a combination of multiresolution image decomposition and color correlation histogram. According to the new algorithm, wavelet coefficients of the image are computed first using a directional wavelet transform. We propose the use of 2D Gabor functions since they achieve the theoretical limit for conjoint resolution on information in the 2D spatial and 2D Fourier domains. A quantization step is then applied before computing one-directional autocorrelograms of the wavelet coefficients. Finally, index vectors are constructed using these one-directional wavelet correlograms. The retrieval results obtained by application of our new method on a 1000 image database demonstrated a significant improvement in effectiveness and efficiency compared to the indexing and retrieval methods based on color correlogram or wavelet transform.

Wavelet Correlogram: A New Approach for Image Indexing and Retrieval

Abstract

In this paper, a new algorithm for content-based image indexing and retrieval is presented. The proposed method is based on a combination of multiresolution image decomposition and color correlation histogram. According to the new algorithm, wavelet coefficients of the image are computed first using a directional wavelet transform such as Gabor wavelets. A quantization step is then applied before computing one-directional autocorrelograms of the wavelet coefficients. Finally, index vectors are constructed using these one-directional wavelet correlograms. The retrieval results obtained by application of our new method on a 1000 image database demonstrated a significant improvement in effectiveness and efficiency compared to the indexing and retrieval methods based on image color correlogram or wavelet transform.

Keywords: Color Correlogram, Wavelet Transform, Image Indexing and Retrieval, Wavelet Correlogram, Gabor Wavelets.

1. Introduction

Digital image libraries and other multimedia databases have been dramatically expanded in recent years. Storage and retrieval of images in such libraries become a real demand in industrial, medical, and other applications [25]. Content-based image indexing and retrieval (CBIR) is considered as a solution. In such systems, some features are extracted from every picture and stored as an index vector [21]. In retrieval phase, every index is then compared (using a similarity criterion) to find some similar pictures to the query image [9].

Two major approaches including spatial and transform domain based methods can be identified in CBIR systems. The first approach usually uses pixel (or a group of adjacent pixels) features like color and shape. Among all these features, color is the most used signature for indexing [8]. Color histogram [23] and its variations [7] were the first algorithms introduced in the pixel domain. Despite its efficiency, color histogram is unable to carry local spatial information of pixels. Therefore, in such systems retrieved images may have many inaccuracies, especially in large image databases. For these reasons, two variations called image partitioning and regional color histogram were proposed to improve the effectiveness of such systems [3,22]. Color correlogram is a different pixel domain approach which incorporates spatial information with color [11,12]. Color-spatial schemes like color correlogram offer more effectiveness in comparison with color histogram methods with little efficiency reduction. Despite the achieved advantage, they suffer from sensitivity to scale, color and illumination changes. Edge orientation autocorrelogram [15] was an effort to reduce the sensitivity of color correlogram method to color and illumination variations. Shape based and color-shape based systems using snakes [10], contour images [19] and other boundary detection methods [15,20], were also proposed as pixel domain methods. These systems are more sensitive to semantic information but have large computational cost.

In the second approach, transformed data are used to extract some higher-level features [2]. Wavelet based methods, which provide better local spatial information in transform domain have been used [14,17,24]. Daubechies' wavelets are the most used in CBIR, because of their fast computation and regularity. In [17], Daubechies' wavelets in three scales were used to obtain transformed data. Then, histograms of wavelet coefficients in each sub-band were computed and stored to construct indexing feature vectors. In SIMPLIcity [14], the image is first classified into different semantic classes using a kind of texture classification algorithm. Then, Daubechies' wavelets are used to extract feature vectors. This method is highly sensitive to color. Shape based indexing method in transform domain has also been proposed for image indexing. Balmelli and Mojsilovic [2] extracted wavelet domain features for the construction of indexing feature vectors.

This paper is an extension of our preliminary work [1] on taking advantage of both pixel and transform domain information. In the present work, we introduce a new approach for image indexing called *wavelet correlogram*. According to this approach, wavelet coefficients are computed first to decompose space-frequency information of the image. These directional sub-bands enable us to compute the image spatial correlation in a more efficient way, while taking into consideration the semantic image information. A quantization step is then applied before computing directional autocorrelograms of the wavelet coefficients. Finally, index vectors are constructed using these wavelet correlograms. Our methodology is novel in the following ways:

- Unlike the methods described in [11,12] and [15], our method is independent of image scaling. Our hybrid image indexing method combines wavelet transform domain data with spatial pixel domain correlation information.
- By applying directional wavelet transforms like Gabor wavelets, we are able to reduce the sensitivity of the indexing retrieval algorithm to image rotation compared to edge orientation autocorrelogram [15] and wavelet transform [14,17] methods.
- Wavelet correlogram is computed using one-dimensional autocorrelograms of the wavelet coefficients. This helps to have a fairly reasonable computational cost in contrast with the color corrlogram method [11].

The proposed algorithm was tested on a 1000 color image database including 10 different image categories. Experimental results demonstrated the improvement in effectiveness and efficiency of the novel method compared to the methods based on wavelet transform or color correlogram.

The organization of the paper is as follows. In section 2, a brief review of the color correlogram method is given. Section 3 presents the wavelet correlogram approach. A short discussion on the choice of appropriate wavelet transform is also given in this section. In section 4, an indexing algorithm based on wavelet correlogram is presented. Experimental results and discussion are given in section 5. Finally, our conclusions and directions for future works are presented in section 6.

2. Color Correlogram

Color correlogram, introduced by Huang *et al*. [11], is an approach for CBIR. Color correlogram of an image is a three dimensional matrix whose elements $\gamma(i, j, k)$ represent the probability of finding two pixels in the image with color c_i and c_j placed in a distance k of each other. Color correlogram expresses how the spatial correlation of pairs of colors changes with distance. This type of feature turns out to be robust in tolerating large

variations in appearance of the same scene caused by changes of viewing position, background and partial occlusions [11].

Let $\mathbf{I}$ be an $N \times N$ image (a square image for simplicity) consisting of M different colors $c_1, c_2, ..., c_M$. For a pixel $p_{(x,y)} \in \mathbf{I}$, let $\mathbf{I}_{(p)}$ expresses the pixel color and $\mathbf{I}_c = \{p | \mathbf{I}_{(p)} = c\}$. Therefore, $p \in \mathbf{I}_c$ is equivalent to $p \in \mathbf{I}, \mathbf{I}_{(p)} = c$. For simplicity, $L_\infty - Norm$ is used to measure the distance between pixels. This measure is computed for two pixels $p_1(x_1, y_1), p_2(x_2, y_2)$ as follows:

$$|p_1 - p_2| = \max\{|x_1 - x_2|, |y_1 - y_2|\} \tag{1}$$

Assume that k is a specified distance and $i, j \in \{1, ..., M\}$. The correlogram of $\mathbf{I}$ is defined by:

$$\gamma(i, j, k) = \Pr_{p_1, p_2 \in \mathbf{I}} \{(p_1, p_2) | p_1 \in \mathbf{I}_{c_i}, p_2 \in \mathbf{I}_{c_j}, |p_1 - p_2| = k\} \tag{2}$$

According to Eq. (2), $\gamma(i, j, k)$ denotes the probability of finding pixels with color c_j at the distance k of the pixel with color c_i. The size of the color correlogram matrix is $M^2 \times K$, where K represents the number of different distances.

2.1 Autocorrelogram

The autocorrelogram of $\mathbf{I}$ represents spatial correlation between identical colors and is defined by:

$$\alpha(i, k) = \gamma(i, i, k) \tag{3}$$

This information is a subset of the color correlogram and requires only $M \times K$ space. Furthermore, it can be computed much faster than Eq. (2). Figures 1(a) and (b) show two different binary images ($M = 2,\ N = 7$). Figures 1(c) and (d) compare the autocorrelogram coefficients computed in both images corresponding to black and white colors, respectively. As illustrated, both images have the same histograms but completely different autocorrelograms.

(Figure 1)

The main advantages of using color correlogram are: *i)* taking into consideration the spatial correlation of colors, *ii)* being easy to implement, and *iii)* producing fairly small size index.

3. Wavelet Correlogram Approach

One of the most important properties of wavelet transform is space-frequency decomposition of the input signal [16]. This property enables us to apply pixel domain tools, such as color correlogram, to the wavelet coefficients of an image. A wavelet correlogram expresses how the spatial correlation of pairs of wavelet coefficients changes with distance. Therefore, the multiscale-multiresolution property of the wavelet transform and TR[1] invariancy of color correlogram are combined. Consequently, the image indexes obtained by the wavelet correlogram method may have better discriminative performance. Among different wavelet decomposition algorithms, the 2D Gabor wavelet has special properties, which make it an appropriate wavelet transform to be used in the wavelet correlogram algorithm. In the following subsections, after a brief review of the 2D Gabor wavelet transform, theoretical development of the wavelet correlogram approach for image indexing and retrieval will be presented.

3.1. Construction of Gabor wavelets

A 2D Gabor function is a Gaussian modulated by a complex sinusoid. It can be specified by the frequency of the sinusoid ω and the standard deviations σ_x and σ_y of the Gaussian envelope as follows [4]:

$$\psi(x,y)=\frac{1}{2\pi\sigma_x\sigma_y}e^{\left[-\frac{1}{2}\left(\frac{x^2}{\sigma_x^2}+\frac{y^2}{\sigma_y^2}\right)+2\pi j\omega x\right]} \tag{4}$$

Two-dimensional Gabor wavelets that satisfy the wavelet theory have been obtained as [13]:

$$\psi_{\omega,\theta}(x,y)=\frac{\omega}{\sqrt{2\pi}\kappa}e^{-\frac{\omega^2}{8\kappa^2}\left(4(x\cos\theta+y\sin\theta)^2+(-x\sin\theta+y\cos\theta)^2\right)}\cdot\left[e^{j(\omega x\cos\theta+\omega y\sin\theta)}-e^{-\frac{\kappa^2}{2}}\right] \tag{5}$$

where, ω is the radial frequency in radians per unit length and θ is the wavelet orientation in radians. The Gabor wavelet is centered at $(x=0,y=0)$ and the normalization factor is such that $\langle\psi,\psi\rangle=1$, i.e. normalized by L^2 norm. κ is a constant, with $\kappa\approx\pi$ for a frequency bandwidth of one octave and $\kappa\approx 2.5$ for a frequency bandwidth of 1.5 octaves. It has been demonstrated that the 2D Gabor functions are local spatial bandpass filters that achieve the theoretical limit for conjoint resolution on information in the 2D spatial and 2D Fourier domains [4]. Examples of Gabor wavelets according to Eq. (5) are shown in Fig. (2).

1. Translation and Rotation

(Figure 2)

Gabor functions do not result in an orthogonal decomposition [13], which means that a wavelet transform based upon the Gabor wavelet is redundant. Manjunath and Ma [18] proposed a design strategy to project the filters so as to ensure that the half-peak magnitude supports of the filter responses in the frequency spectrum touch one another. By doing this, it can be ensured that the filters will capture the maximum information with minimum redundancy [6]. The Gabor wavelets are obtained by dilation and rotation of the generating function $\psi(x, y)$ using:

$$\psi_{m,n}(x,y) = a^{-m}\psi\left[a^{-m}(x\cos\theta + y\sin\theta), a^{-m}(x\sin\theta + y\cos\theta)\right] \tag{6}$$

where, $\theta = \frac{n\pi}{K_\theta}$, K_θ is the number of orientations desired and $m, n \in \mathbf{Z}$ represent scale and orientation, respectively. The scale factor a^{-m} is meant to ensure that the energy is independent of m. Equation (6) can be written in the frequency domain as:

$$\psi(u,v) = \frac{1}{2\pi\sigma_u\sigma_v} e^{\left\{-\frac{1}{2}\left[\frac{(u-\omega)^2}{\sigma_u^2} + \frac{v^2}{\sigma_v^2}\right]\right\}} \tag{7}$$

where, $\sigma_u = 1/2\pi\sigma_x$ and $\sigma_v = 1/2\pi\sigma_y$. The resulted real-valued even symmetric Gabor filters, which are oriented over a range of 180°, are more appropriate for image indexing purposes [18]. Examples of Gabor filters in the frequency domain according to Eq. (7) are shown in Fig. (3).

(Figure 3)

3.2. Wavelet correlogram

Let $\mathbf{W}^{m,n}(x, y)$ be a $N \times N$ matrix (a square matrix for simplicity) representing the 2D Gabor wavelet transform of an input image $\mathbf{I}$ of size $N \times N$ corresponding to the bandwidth $m \in \{1, ..., S\}$ and direction $n \in \{1, ..., K_\theta\}$. We assume that the wavelet coefficients $\mathbf{W}^{m,n}$ are quantized into L levels w_1, …, w_L. For a pixel $p = (x, y) \in \mathbf{W}^{m,n}$, let $\mathbf{W}^{m,n}(p)$ denote its level. Let $\mathbf{W}_l^{m,n} = \left\{ p \mid \mathbf{W}^{m,n}(p) = l \right\}$. Therefore,

$p \in \mathbf{W}_{l}^{m,n}$ is equivalent to $p \in \mathbf{W}^{m,n}$, $\mathbf{W}^{m,n}(p) = l$. The distance between pixels $p_1 = (x, y)$, $p_2 = (\xi, \eta)$ $\xi, \eta \in \mathbf{R}$, along the direction n is defined by:

$$\left| p_1 - p_2 \right|_n = \max\left\{ \left| x_1 - [\xi] \right|, \left| y_1 - [\eta] \right| \right\} \tag{8}$$

where, $[.]$ represents the integer part.

Assume that k is a specified distance and $i, j \in \{1, ..., L\}$. The wavelet correlogram of $\mathbf{I}$ corresponding to its wavelet transform in the bandwidth m and the direction n is defined by:

$$\gamma^{m,n}(i, j, k) = \Pr_{p_1 \in \mathbf{I}}\left\{ (p_1, p_2) \middle| p_1 \in \mathbf{W}_{l_i}^{m,n}, p_2 \in \mathbf{W}_{l_j}^{m,n}, \left| p_1 - p_2 \right|_n = k \right\} \tag{9}$$

where p_1 and p_2 have integer and real coordinates, respectively and the level associated to p_2 may be computed by some kind of interpolation technique. According to Eq. (9), $\gamma^{m,n}(i, j, k)$ denotes the probability of finding pixels with level l_j at the distance k of the pixel with level l_i in the wavelet coefficient matrix corresponding to the bandwidth m and direction n. The size of the wavelet correlogram matrix for each pair of (m, n) is $L^2 \times K$, where K represents the number of different distances. The wavelet correlogram computing equations for each pair of (m, n) are:

$$\Gamma^{m,n}(i, j, k) = \left\{ p_1 \in \mathbf{W}_{l_i}^{m,n}, p_2 \in \mathbf{W}_{l_j}^{m,n} \middle| \left| p_1 - p_2 \right|_n = k \right\} \tag{10}$$

$$\gamma^{m,n}(i, j, k) = \frac{\left| \Gamma^{m,n}(i, j, k) \right|}{2 \cdot h_{l_i}\left(\mathbf{W}^{m,n} \right)} \tag{11}$$

where, $\left| \Gamma^{m,n}(i, j, k) \right|$ in Eq. (11) represents the size of $\Gamma^{m,n}(i, j, k)$, and $h_{l_i}(\mathbf{W}^{m,n})$ in the denominator is the total number of pixels of level l_i:

$$h_{l_i}(\mathbf{W}^{m,n}) = N^2 \cdot \Pr\left\{ p \in \mathbf{W}_{l_i}^{m,n} \right\} \tag{12}$$

Direct computation of color correlogram according to Eq. (2) takes $O\left(N^2 K^2\right)$ time per each pair of colors [11]. In the same way, direct computation of wavelet correlogram for all scales and directions according to Eq.

(11) takes $O\left(SK_\theta N^2 K\right)$ time per each pair of wavelet coefficient quantized levels. Although it seems that the computational cost of the wavelet correlogram is larger, the following remarks result in a different conclusion:

- In practice, S and K_θ are fairly small (≤ 4). Our experiments using small values for S and K_θ demonstrated a good overall performance of the indexing retrieval algorithm.
- Because of multiscale property of the wavelet correlogram, the maximum number of distances (K) is generally smaller than the maximum number of distances used by the color correlogram indexing algorithm.
- The number of quantized levels are, in general, less than the number of image colors (gray levels). In the experimental results reported in this paper, only 4 quantized levels have been used which is much smaller compared to 256 image gray levels.
- Finally, the data redundancy of Gabor wavelet coefficients, may be exploited in order to reduce the wavelet coefficient matrix dimensions. This issue is currently being studied which may allow further reduction of the computational cost.

3.3. Wavelet autocorrelogram

The wavelet autocorrelogram of $\mathbf{I}$ corresponding to the wavelet coefficients of the image computed in the bandwidth and direction (m,n) represents the spatial correlation between identical levels and is defined by:

$$\alpha^{m,n}\left(i,k\right)=\gamma^{m,n}\left(i,i,k\right) \tag{13}$$

This information is a subset of the color correlogram and requires only $L\times K$ space. Furthermore, it can be computed much faster than Eq. (11). The wavelet autocorrelogram computing equations are:

$$\Gamma^{m,n}\left(i,i,k\right)=\left\{\left(p_1,p_2\right)\middle|\, p_1,p_2\in \mathbf{W}_{l_i}^{m,n},\left|p_1-p_2\right|_n=k\right\} \tag{14}$$

$$\alpha^{m,n}(i,k)=\frac{\left|\Gamma^{m,n}\left(i,i,k\right)\right|}{2\cdot h_{l_i}\left(\mathbf{W}^{m,n}\right)} \tag{15}$$

where, $\left|\Gamma^{m,n}(i,i,k)\right|$ in Eq. (15) represents the size of $\Gamma^{m,n}(i,i,k)$. Because of multiscale property of the wavelet autocorrelogram, a smaller value of K is sufficient to capture the spatial correlation compared to the color autocorreolgram method.

Figures 4(a) and (b) show two binary images ($M = 2,\ N = 32$) with the same histograms. Figures 4(c) and (d) compare the autocorrelograms of two images computed over 5 different distances ($K = 5$). As illustrated, the autocorrelograms are approximately similar. Therefore, a larger number of distances should be used in order to obtain a significant difference between autocorrelograms. Figures 4(e) and (f) compare the wavelet autocorrelograms computed using the third scale ($m = 3$) wavelet coefficients in horizontal ($n = 1$) and vertical ($n = 2$) directions. In this example, the wavelet coefficients were quantized into only two levels (levels 1 and 2). As may be observed, there is significant difference between wavelet autocorrelograms in the third wavelet resolution.

(Figure 4)

The main advantages of using wavelet correlogram are: *i)* taking into consideration the spatial correlation of wavelet coefficients which is related to spatial correlation of colors in the image, *ii)* describing the global distribution of local spatial correlation of wavelet coefficients, *iii)* being less sensitive to changes in color values, *iv)* providing scale invariancy of the image indexing algorithm *v)* providing rotation invariancy by using directional Gabor wavelet transform, *vi)* being easy and efficient to implement, and *vii)* producing fairly small size index.

4. Wavelet Correlogram Indexing Algorithm

Figure (5) illustrates three major parts of the wavelet correlogram indexing algorithm, including preprocessing, processing and feature construction phases. According to the wavelet correlogram indexing algorithm, the wavelet transform of the input image is computed first. In the second step, the computed wavelet coefficients are quantized to a limited number of levels. Then, one-dimensional autocorrelograms of directional quantized wavelet coefficients are computed. Finally, one-dimensional autocorrelograms are used to form feature vectors for image indexing.

(Figure 5)

4.1. Preprocessing

The preprocessing phase is principally aimed to prepare images in the database for further processing. The image database is composed of 1000 color images in different sizes and different input data formats. Color

pictures in the database are first transformed to a unified gray level format. This transform is primarily aimed to reduce the input data dimensionality while preserving the maximum image information content. For this purpose, the RGB values are first converted to NTSC coordinates, and after setting the hue and saturation components to zero, the values are converted back to RGB color space.

4.2. Gabor wavelet transform

In practice, a limited number of scales and orientations are sufficient for wavelet decomposition. According to our experiments, applying wavelet transform in three scales gives a good compromise between efficiency and effectiveness of the algorithm. The experimental results reported in the next section have been obtained using wavelet transform in three scales and two directions. A comprehensive performance study is currently being made in order to optimize the wavelet decomposition parameters. This study concerns also the data redundancy of wavelet coefficients, which is an important issue for reducing the overall computational cost of the algorithm.

4.3. Quantization of wavelet coefficients

Wavelet coefficients are real numbers with a large dynamic range. A quantization step is therefore required before computing the wavelet autocorrelogram. To take into consideration the dynamic range of wavelet coefficients, we use different quantized levels in each wavelet transform resolution. Figure (6) shows the quantization procedure performed on 3 consecutive scales of wavelet transform. In each scale, small coefficients around zero are considered as noise and discarded. For the results presented in the next section, we used 4 quantized levels in each scale of the wavelet transform. These quantized levels were obtained experimentally, by dividing the dynamic range into 4 bins, each bin representing approximately 25% of wavelet coefficients population (Fig. 6).

(Figure 6)

4.4. Wavelet correlogram computation

Wavelet correlogram represents the spatial correlation of wavelet coefficients of an image. In this section, we introduce a particular scheme for the computation of wavelet correlogram, mainly based on wavelet coefficients in horizontal and vertical directions. It should be noted that the proposed procedure may be easily generalized in order to be used in any directional wavelet transform such as Gabor wavelets.

Wavelet coefficients computed using horizontal (vertical) filters correspond to low pass and high pass filtering in horizontal (vertical) and vertical (horizontal) directions, respectively. Logically, the wavelet autocorrelogram is computed only in the direction of low-pass filtering. Consecutively, one-dimensional horizontal and vertical autocorrelograms are computed on horizontal and vertical matrices, respectively. This method has less computational cost compared to the two-dimensional autocorrelogram proposed by Huang *et al.* [11]. The same procedure may be used in diagonal directions if wavelet decomposition has been made in these directions.

4.5. Feature vector structure

A simple feature vector structure has been used for the experimental results presented in this paper. It consists of 96 real numbers computed using one-dimensional version of Eq. (6). According to Fig. (6), the wavelet coefficients are quantized into four levels in each scale. By computing the autocorrelogram in four distances ($k = 1,...,4$), we obtain 16 real numbers for each wavelet coefficient matrix. Using two matrices (horizontal and vertical) per scale and three consecutive scales, result in 96 total real numbers, equivalent to 384 bytes per feature vector.

5. Results and Discussion

For evaluation of the proposed algorithm, a number of query images were selected randomly from a 1000 image subset of the COREL database[1]. The images in the database have different sizes and are categorized in 10 classes as listed in Table (1). Each class contains 100 pictures in JPEG format. Within this database, it is known whether any two images are of the same category. In particular, a retrieved image is considered a match if and only if it is in the same category as the query. This assumption is reasonable, since the 10 categories were chosen so that each depicts a distinct semantic topic. Every image in the database was tested as a query and the retrieval ranks of all the rest images were recorded. Figure (7) illustrates four query results of our indexing-retrieval program developed based on the wavelet correlogram algorithm. The graphic user interface (GUI) of the indexing-retrieval program enables the user to enter the query image and the desired number of retrieved images. Moreover, the user can select the retrieval coefficients (weights) corresponding to each wavelet resolution level in order to obtain the best result. In the examples illustrated in Fig. (7), the same coefficients were selected for all three resolution levels. Each query results in a preselected number of retrieved images which are illustrated and listed in ascending order according to the Euclidean distance

2. From SIMPLIcity site http://wang.ist.psu.edu/docs/related/

between indexing vectors of the query and retrieved images. Finally, the retrieval precision is reported in the lower right-hand corner of the GUI .

(Figure 7)

A number of statistics were computed for each query. Let $Y(Q)$ be the set of retrieved images which are matched to the query image Q:

$$Y(Q) = \left\{ \mathbf{I}_i \middle| rank(\mathbf{I}_i) \prec N, \mathbf{I}_i \in A \right\} \tag{16}$$

where, N is the number of retrieved images and A is the subset of image database having the same category as the query image. Five performance criteria were used for evaluation of the image indexing and retrieval algorithm: *i)* the precision, *ii)* weighted precision, *iii)* rank, *iv)* standard deviation of the precision, and *v)* standard deviation of the rank. The precision of the N retrieved images, for a query image Q is computed as follows:

$$P(Q) = \frac{\left|Y(Q)\right|}{N} \tag{17}$$

where, $\left|\mathrm{Y(Q)}\right|$ represents the size of $Y(Q)$. The weighted precision is computed using:

$$WP(Q) = \frac{1}{N} \sum_{k=1}^{N} \frac{n_k}{k} \tag{18}$$

where n_k represents the number of matches between the first k retrieved images. $P(Q)$ and $WP(Q)$ are always between 0 and 1. The rank for every query image Q is computed over all matches using the following equation:

$$R(Q) = \frac{1}{N_A} \sum_{i=1}^{N_A} rank(\mathbf{I}_i) \qquad , \qquad \forall I_i \in A \tag{19}$$

where, N_A represents the number of images in the same category as the query image. The average of the precision, weighted precision and rank are defined as:

$$P = \frac{1}{N_q} \sum_{k=1}^{N_q} P(\mathbf{I}_k) \tag{20}$$

$$WP = \frac{1}{N_q}\sum_{k=1}^{N_q} WP(\mathbf{I}_k) \tag{21}$$

$$R = \frac{1}{N_q}\sum_{k=1}^{N_q} R(\mathbf{I}_k) \tag{22}$$

where N_q represents the number of queries and $\mathbf{I}_k$ represents the k th image in the database. For a global averaging, N_q is equal to the total number of images in the database. For averaging in a specified category, N_q is equal to the number of images in the specified category. The standard deviation of the precision and rank are defined as:

$$STD(P) = \sqrt{\frac{1}{N_q - 1}\sum_{k=1}^{N_q} (P(\mathbf{I}_k) - P)^2} \tag{23}$$

$$STD(R) = \sqrt{\frac{1}{N_q - 1}\sum_{k=1}^{N_q} (R(\mathbf{I}_k) - R)^2} \tag{24}$$

For a system that ranks images randomly, the average precision and weighted precision are about 0.1, and the average rank is about N/2, where N is the total number of images in the database. An ideal CBIR system should demonstrate average precision and weighted precision of 1 and an average rank of $N_A/2$, where N_A is the number of images in a specified category.

Table (1) shows the quantitative results obtained by the application of the algorithm to the database. A total average of 71% matched retrieved images is achievable using the wavelet correlogram indexing retrieval algorithm. The same experiment, performed using wavelet based or color correlogram based methods (Table 2), demonstrated lower performance on average precision and weighted precision.

(Table 1)

Figure (8) compares the wavelet correlogram with SIMPLIcity [14] and color histogram [7] methods on average precision P, average rank of the matched images R, and the standard deviation of the ranks of the matched images STD(R). The lower numbers indicate better results for the last two plots.

(Figure 8)

Table (2) compares the results obtained by the wavelet correlogram algorithm with the results of the wavelet based and color correlogram based methods. WBIIS [24] and SIMPLIcity [5,14] are mainly based on wavelet transform, while color correlogram [11] uses color correlation and edge correlogram [15] uses edge correlation. Columns 4-7 compare the space requirements for storage of the feature vectors, the retrieval computational costs and the total average retrieval precision and weighted precision, respectively. As illustrated, the wavelet correlogram method has a fairly small size feature vector and reasonable computational cost, while demonstrating higher average retrieval accuracy.

(Table 2)

5. Concluding Remarks

In this paper, a new approach in CBIR was presented. Two different tools from pixel and transform domains were combined to develop a new algorithm called wavelet correlogram. Primary results were promising and demonstrated higher performance (in effectiveness and efficiency) of the new method compared to the methods based on each domain individually. The index vector using wavelet correlogram is fairly small and independent of the picture size.

Further developments should be made in order to optimize the proposed method. A simple quantization scheme has been used in the presented work. Increasing the number of quantized levels and using more appropriate thresholds may help to obtain better results. Feature vector structure may also be modified to reduce its size and improve its discriminative property. In retrieval phase, using non-Euclidean distances such as relative distance [11] may improve the retrieval performance. Moreover, it is shown that using different coefficients for each wavelet resolution level may have a considerable effect on the retrieval accuracy. An optimized procedure is currently being developed using genetic algorithms in order to determine the best set of coefficients to be used in retrieval phase for each resolution level.

References

1. H. Abrishami Moghaddam, A. H. Rouhi, T. Taghizadeh Khajoie, "Wavelet Correlogram: A New Algorithm for Image Indexing and Retrieval Using Wavelet Correlogram", *Proc. of 16th IEEE International Conference on Image Processing ICIP2003,* Vol. 3, pp. 497-500, Barcelona, Spain, Sep. 2003.

2. L. Balmelli, A. Mojsilovic, "Wavelet Domain Features for Texture Description, Classification and Replicability Analysis", in *Wavelets in Signal and Image Analysis: From Theory to Practice* (edited book), Kluwer Academic Publishers.

3. C. Carson, M. Thomas, S. Blongie, J.M. Hellerstine, and J. Malik, "Blobworld: a system for Region-Based Image Indexing and Retrieval", *Proc. of SPIE Visual Information Systems,* pp. 509-516, June 1999.

4. J. G. Daugman, "Uncertainty Relation for Resolution in Space, Spatial frequency, and Orientation Optimized by Two-Dimensional Visual Cortical Filters", *Journal of Optical Society of America*, Vol. 2, No. 7, pp. 1,160-1,169, 1985.

5. Y. Du, J. Z. Wang, "A scalable integrated region-based image retrieval system", *Proc. of 14th IEEE International Conference on Image Processing ICIP2001*, pp. 22-25, Thessaloniki, Greece, Oct. 2001.

6. R. J. Ferrari, R. M. Rangayyan, J. E. L. Desautels, A. F. Frère, "Analysis of Asymmetry in Mammograms via Directional Filtering With Gabor Wavelets", *IEEE Trans. on Medical Imaging*, Vol. 20, No. 9, pp. 953-964, Sep. 2001.

7. M. Flickner, H. Sawhney, W. Niblack, J. Ashley, Q. Hunag, B. Dom, M. Gorkani, J. Hafner, D. Lee, D. Petkovic, D. Steele, P. Yanker, "Query by Image and Video Content: The QBIC System", IEEE Computer, vol. 28, No. 9, pp. 1995.

8. Th. Gevers, "Color Based Image Retrieval", Multimedia Search, Ed. M. Lew, Springer-Verlag, Jan. 2001.

9. V. N. Gudivada, J. V. Raghavan, "Content-based image retrieval systems", *IEEE Computer Magazine,* Vol. 28, No. 9, pp. 18-22, Sep. 1995.

10. Ip. H. H. S. and D. Shen, "An affine-invariant active contour model (AI-snake) for model-based segmentation", *Image and Vision Computing*, Vol.16, No.2, pp. 135-146, Japan, Apr. 1998.

11. J. Huang, S. R. Kumar, M. Mitra, W. J. Zhu, R. Zabih, "Image Indexing Using Color correlograms", *IEEE Conf. Comp. Vision and Pattern Recognition*, pp. 762-768, San Juan, 1997.

12. J. Huang, S.R. Kumar, M. Mitra, W. J. Zhu, R. Zabih, "Spatial color indexing and applications", *International Journal of Computer Vision,* Vol. 35, No. 3, pp. 245-268, 1999.

13. T.S. Lee, "Image Representation Using 2D Gabor Wavelets", IEEE Trans. On Pattern Analysis and Machine Intelligence, Vol. 16, No. 10, Oct. 1996.

14. J. Li., J. Z. Wang, G. Wiederhold, "SIMPLIcity: Semantics-sensitive Integrated Matching for Picture Libraries", *IEEE Trans. on Pattern Analysis and Machine Intelligence,* Vol. 23, No. 9, pp. 947-963, Sep. 2001.

15. F. Mahmoudi, J. Shanbehzadeh, A.M. Eftekhari-Moghadam H. Soltanian-Zadeh, "Image retrieval based on shape similarity by edge orientation autocorrelogram", *Pattern Recognition,* Vol. 36, No. 2, pp. 1725-1736, Aug. 2003.

16. S. Mallat, *A wavelet tour of signal processing*, *2nd Edition*, Academic Press, 1999.

17. M. K. Mandal, S. Panchanathan, and T. Aboulnasr, "Fast Wavelet Histogram Techniques for Image Indexing", *Journal of Computer Vision and Image Understanding,* Vol. 75, No. 1/2, pp. 99-110, July/Aug. 1999.

18. B. S. Manjunath, W.Y. Ma, "Texture features for browsing and retrieval of image data", IEEE Trans. Pattern Anal. Machine Intell., Vol. 18, pp. 837-842, Aug. 1996.

19. A. Quddus, F. Alaya Cheikh, and M. Gabbouj, "Content-based Object Retrieval Using Maximum Curvature Points In Contour Images", *Proc. of SPIE/EI'2000 Symposium, on Storage and Retrieval for Media Databases,* 2000.

20. A. Sajjanhar and G. Lu, "A grid based shape indexing and retrieval method", *Special issue of Australian Computer Journal on Multimedia Storage and Archiving Systems*, Vol. 29, No. 4, pp. 131-140, Nov. 1997.

21. A. W. M. Smeulders, M. Worring, S. Santini, A. Gupta, and R. Jain, "Content-Based Image Retrieval at the End of Early Years," *IEEE Trans. on Pattern Analysis and Machine Intelligence,* Vol. 22, No. 12, Dec. 2000.

22. M. Stricker, A. Dimai, "Spectral covariance and fuzzy regions for image indexing", *Machine Vision and Applications,* Vol. 10, pp. 66-73, 1997.

23. M. J. Swain, D. H. Ballard, "Color indexing", *Int. Journal of Computer Vision,* Vol. 7, pp. 11-32. 1991.

24. J. Z. Wang, G. Wiederhold, O. Firschein, S. X. Wei "Content-based image indexing and searching using Daubechies' wavelets," *Int. Journal of Digital Libraries*, vol. 1, no. 4, pp. 311-328, Springer-Verlag, 1998.

25. "Special issue on digital library," *IEEE Trans. Pattern Analysis and Machine Intelligence,* Vol. 18, Aug. 1996.

List of Captions of Figures

Figure 1: (a), (b) Two sample binary images, (c), (d) black and white color autocorrelograms in four distances {1, 2, 3, 4}.

Figure 2: (a) An ensemble of Gabor wavelets (1.5 octave bandwidth) and (b) their coverage of the spatial frequency plane. Each ellipse shows the half-amplitude bandwidth contour dilated by a factor of 2, covering almost the complete support of a wavelet [13].

Figure 3: Examples of Gabor filters in the frequency domain. Each ellipse represents the range of the corresponding filter response from 0.5 to 1.0 in squared magnitude. The plots (a) and (b) illustrate two different ways for sampling the frequency spectrum by changing the U_l, U_h, S and K_θ parameters of the Gabor presentation. (a) $U_l = 0.03$, $U_h = 0.4$, $S = 3$, $K_\theta = 2$, (b) $U_l = 0.05$, $U_h = 0.4$, $S = 3$, and $K_\theta = 4$.

Figure 4: (a), (b) Two sample binary images, (c), (d) black and white color autocorrelograms in four distances {1, 2, 3, 4, 5}. (e), (f) two-level (levels 1 and 2) wavelet correlograms in the third scale of the wavelet transform in horizontal and vertical directions, respectively.

Figure 5: Wavelet correlogram indexing algorithm.

Figure 6: Quantization levels in Horizontal and Vertical directions (a) scale 1, (b) scale 2, and (c) scale 3. Each bin represents approximately 25% of wavelet coefficients population.

Figure 7: Results obtained from query image (a) 314, (b) 593, (c) 621, (d) 924.

Figure 8: Comparing wavelet correlogram with SIMPLIcity and color histogram methods on average precision P, average rank of the matched images R, and the standard deviation of the ranks of the matched images STD(R). The lower numbers indicate better results for the last two plots.

List of Captions of Tables

Table 1: Results of the wavelet correlogram indexing retrieval algorithm.

Table 2: Comparison of different image indexing retrieval systems.

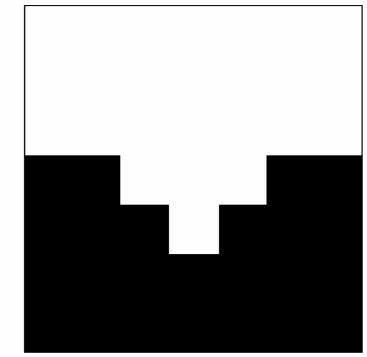

(a)

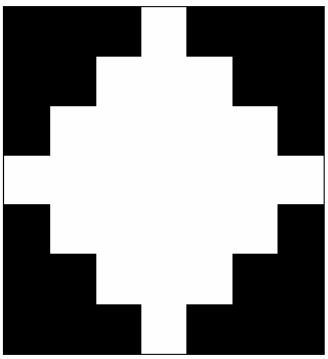

(b)

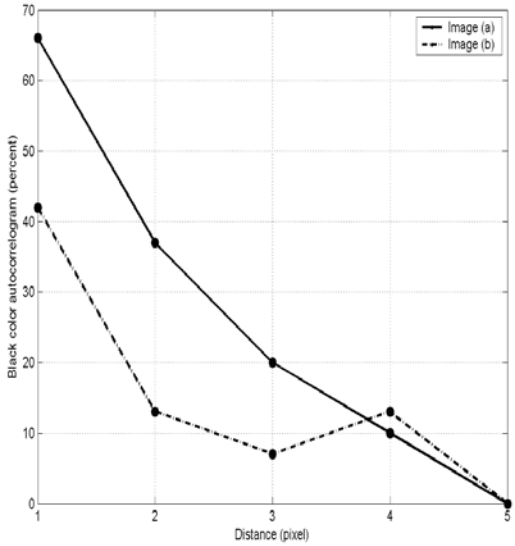
Image (a)
Image (b)
Black color autocorrelogram (percent)
Distance (pixel)
0
10
20
30
40
50
60
70
1
2
3
4
5

(c)

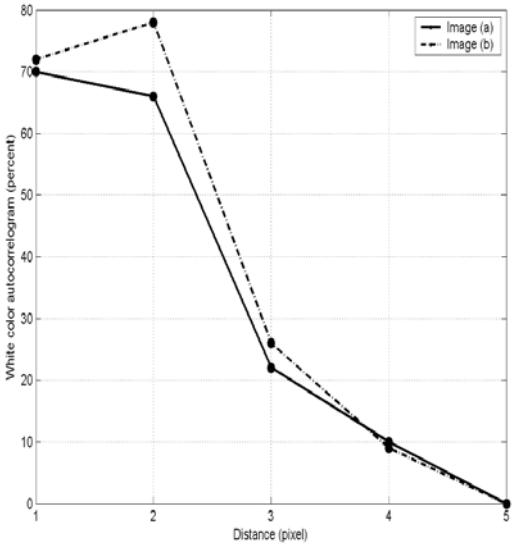
Image (a)
Image (b)
White color autocorrelogram (percent)
Distance (pixel)
0
10
20
30
40
50
60
70
80
1
2
3
4
5

(d)

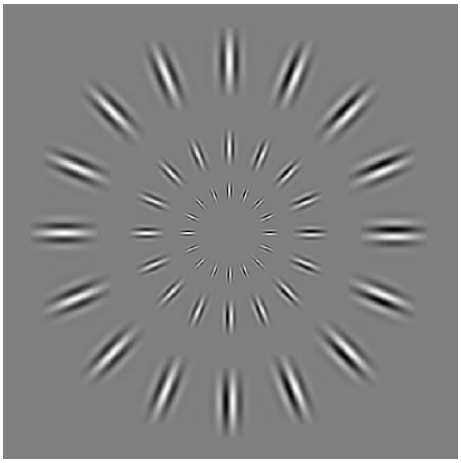

(a)

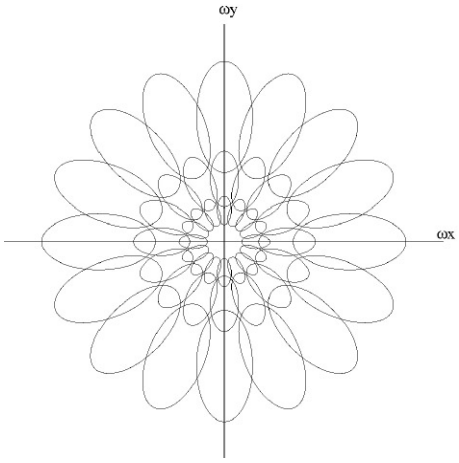

(b)

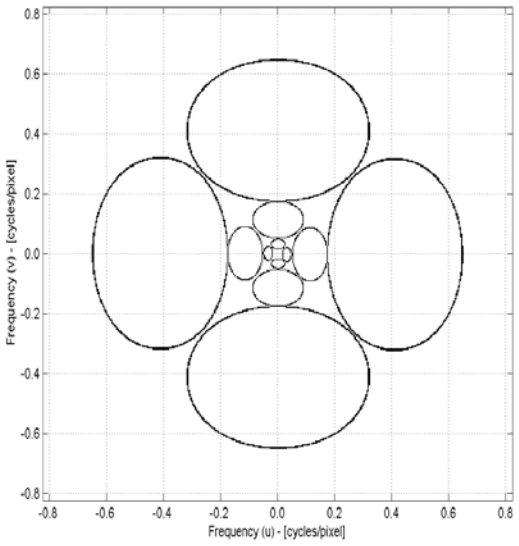
Frequency (v) - [cycles/pixel]
Frequency (u) - [cycles/pixel]
0.8
0.6
0.4
0.2
0
-0.2
-0.4
-0.6
-0.8

(a)

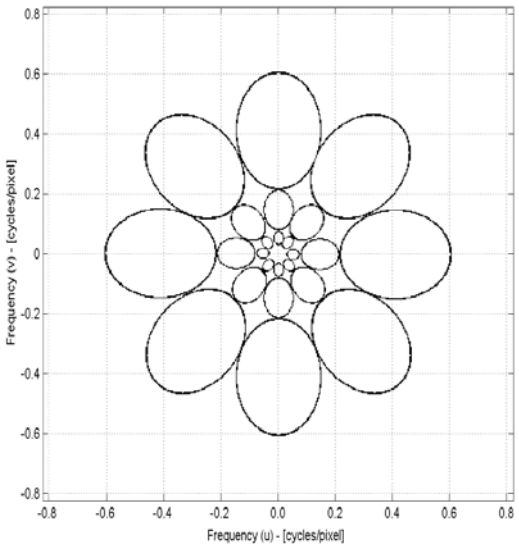
Frequency (v) - [cycles/pixel]
Frequency (u) - [cycles/pixel]
0.8
0.6
0.4
0.2
0
-0.2
-0.4
-0.6
-0.8

(b)

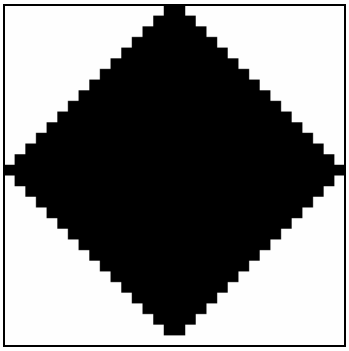

(a)

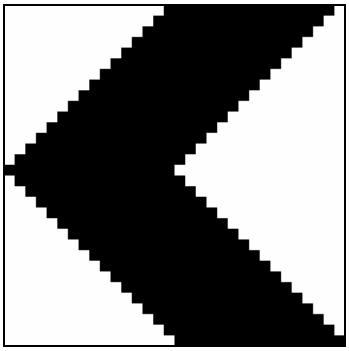

(b)

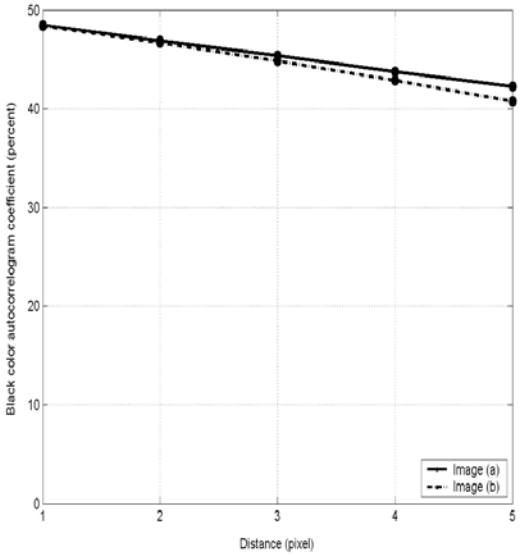
Black color autocorrelogram coefficient (percent)
Distance (pixel)
Image (a)
Image (b)

(c)

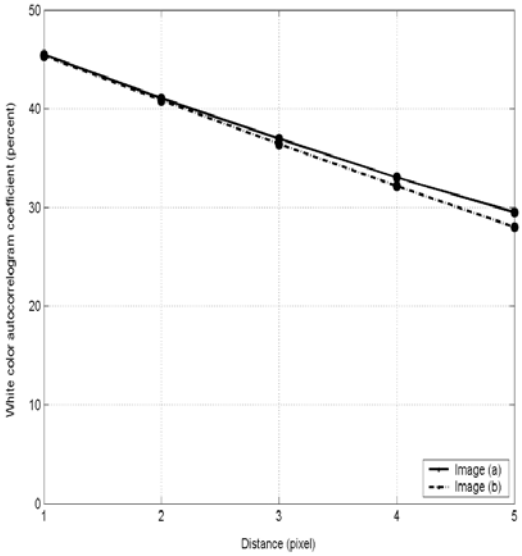
White color autocorrelogram coefficient (percent)
Distance (pixel)
Image (a)
Image (b)

(d)

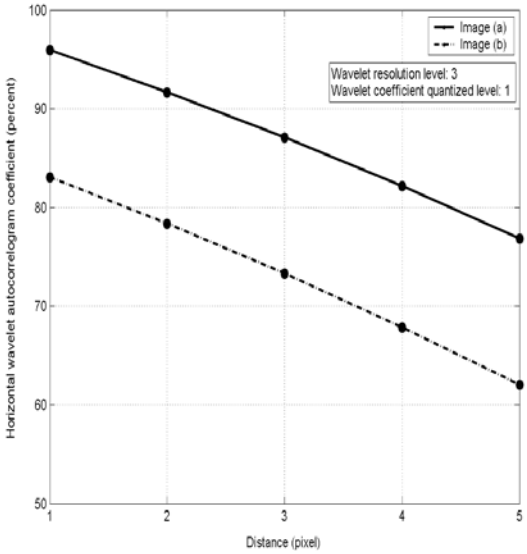
Horizontal wavelet autocorrelogram coefficient (percent)
Distance (pixel)
Image (a)
Image (b)
Wavelet resolution level: 3
Wavelet coefficient quantized level: 1

(e)

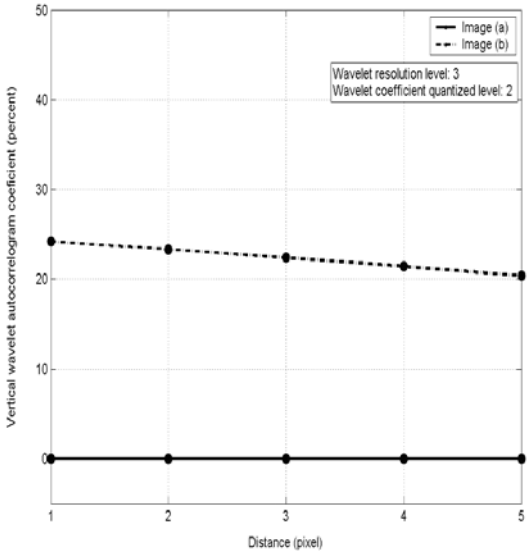
Vertical wavelet autocorrelogram coefficient (percent)
Distance (pixel)
Image (a)
Image (b)
Wavelet resolution level: 3
Wavelet coefficient quantized level: 2

(f)

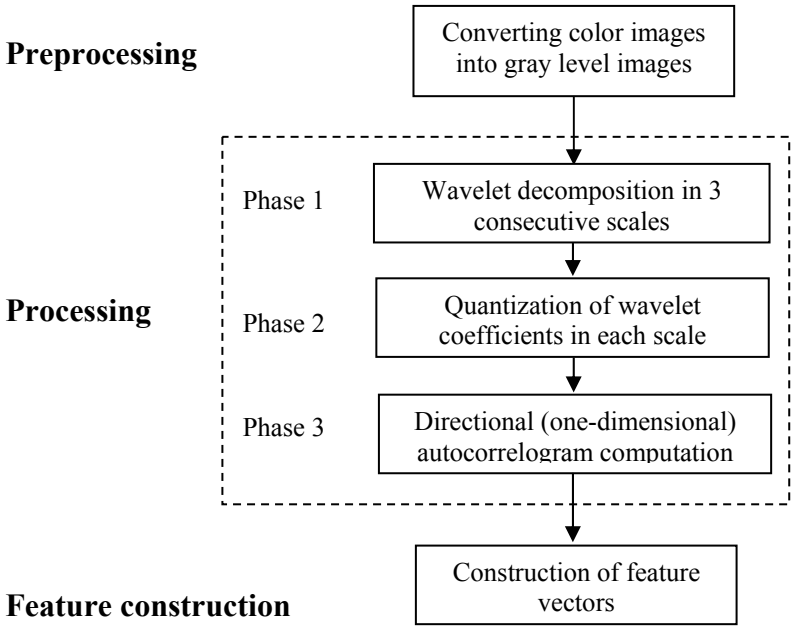
Preprocessing
Converting color images into gray level images
Processing
Phase 1
Wavelet decomposition in 3 consecutive scales
Phase 2
Quantization of wavelet coefficients in each scale
Phase 3
Directional (one-dimensional) autocorrelogram computation
Feature construction
Construction of feature vectors

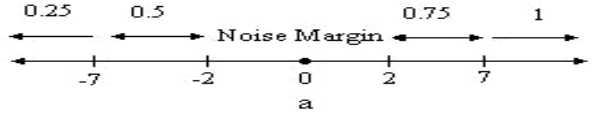
0.25
0.5
Noise Margin
0.75
1
-7
-2
0
2
7

a

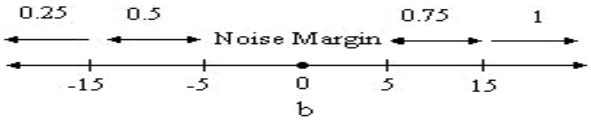
0.25
0.5
Noise Margin
0.75
1
-15
-5
0
5
15

b

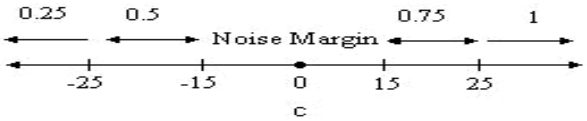
0.25
0.5
Noise Margin
0.75
1
-25
-15
0
15
25

c

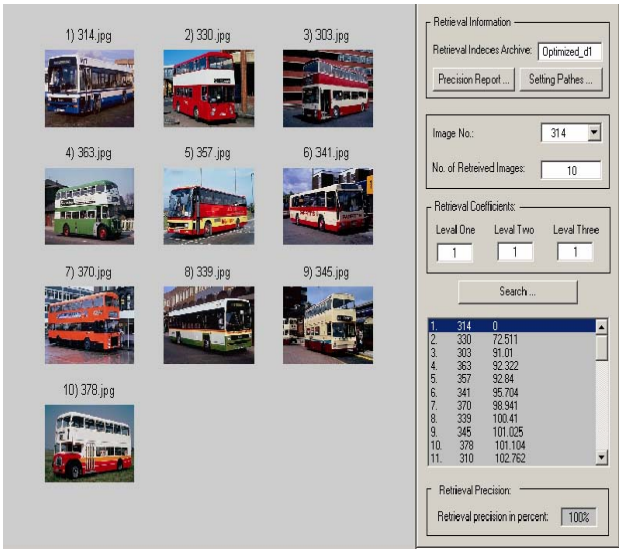
1) 314.jpg
2) 330.jpg
3) 303.jpg
4) 363.jpg
5) 357.jpg
6) 341.jpg
7) 370.jpg
8) 339.jpg
9) 345.jpg
10) 378.jpg
Retrieval Information
Retrieval Indeces Archive: Optimized_d1
Precision Report ...
Setting Pathes ...
Image No.: 314
No. of Retreived Images: 10
Retrieval Coefficients:
Level One Level Two Level Three
1 1 1
Search ...
1. 314 0
2. 330 72.511
3. 303 91.01
4. 363 92.322
5. 357 92.84
6. 341 95.704
7. 370 98.941
8. 339 100.41
9. 345 101.025
10. 378 101.104
11. 310 102.762
Retrieval Precision:
Retrieval precision in percent: 100%

(a)

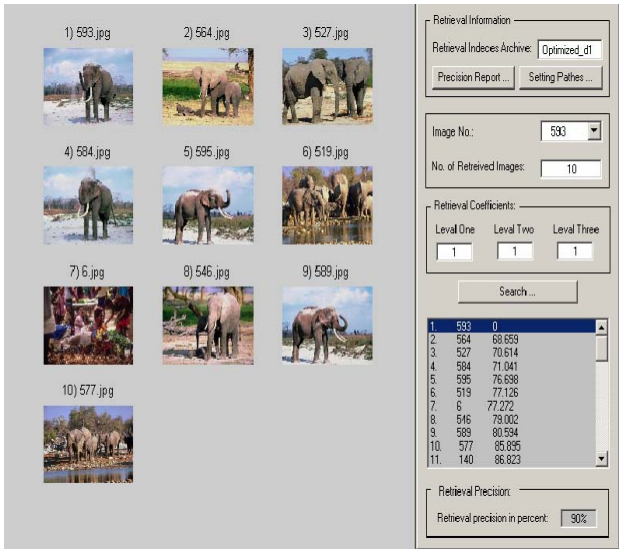
1) 593.jpg
2) 564.jpg
3) 527.jpg
4) 584.jpg
5) 595.jpg
6) 519.jpg
7) 6.jpg
8) 546.jpg
9) 589.jpg
10) 577.jpg
Retrieval Information
Retrieval Indeces Archive: Optimized_d1
Precision Report ...
Setting Pathes ...
Image No.: 593
No. of Retreived Images: 10
Retrieval Coefficients:
Level One Level Two Level Three
1 1 1
Search ...
1. 593 0
2. 564 68.659
3. 527 70.614
4. 584 71.041
5. 595 76.698
6. 519 77.126
7. 6 77.272
8. 546 79.002
9. 589 80.594
10. 577 85.895
11. 140 86.823
Retrieval Precision:
Retrieval precision in percent: 90%

(b)

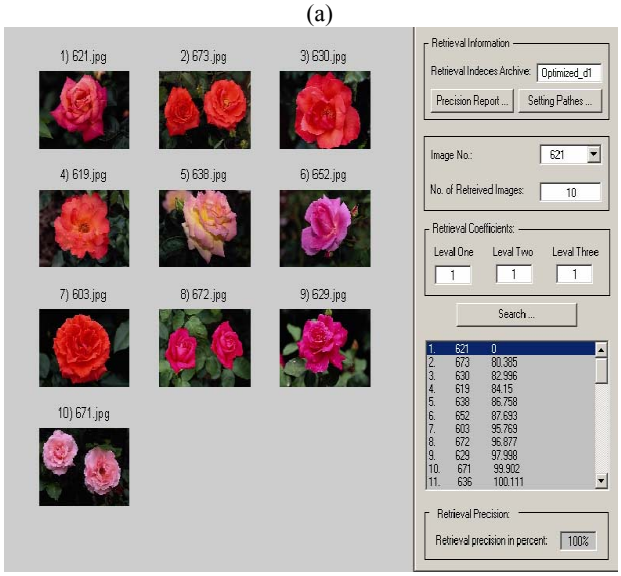
1) 621.jpg
2) 673.jpg
3) 630.jpg
4) 619.jpg
5) 638.jpg
6) 652.jpg
7) 603.jpg
8) 672.jpg
9) 629.jpg
10) 671.jpg
Retrieval Information
Retrieval Indeces Archive: Optimized_d1
Precision Report ...
Setting Pathes ...
Image No.: 621
No. of Retreived Images: 10
Retrieval Coefficients:
Level One Level Two Level Three
1 1 1
Search ...
1. 621 0
2. 673 80.385
3. 630 82.996
4. 619 84.15
5. 638 86.758
6. 652 87.693
7. 603 95.769
8. 672 96.877
9. 629 97.998
10. 671 99.902
11. 636 100.111
Retrieval Precision:
Retrieval precision in percent: 100%

(c)


1) 924.jpg
2) 992.jpg
3) 976.jpg
4) 930.jpg
5) 918.jpg
6) 939.jpg
7) 993.jpg
8) 906.jpg
9) 954.jpg
10) 922.jpg
Retrieval Information
Retrieval Indeces Archive: Optimized_d1
Precision Report ...
Setting Pathes ...
Image No.: 924
No. of Retreived Images: 10
Retrieval Coefficients:
Level One Level Two Level Three
1 1 1
Search ...
1. 924 0
2. 992 53.555
3. 976 56.222
4. 930 58.202
5. 918 58.948
6. 939 66.599
7. 993 67.582
8. 906 68.025
9. 954 68.31
10. 922 69.204
11. 978 70.554
Retrieval Precision:
Retrieval precision in percent: 100%

(d)

Parameter / Category	Average Precision P	STD of Precision STD(P)	Average Weighted Precision (WP)	Rank (R)	STD of Rank STD(R)
Africans	٠,٦٣	0.24	0.72	٢٧٩	69
Beaches	0.61	0.27	0.70	323	128
Buildings	0.59	0.21	0.68	294	120
Buses	0.90	0.17	0.93	117	68
Dinosaurs	0.86	0.20	٠,٨٩	424	61
Elephants	0.64	0.19	0.72	249	72
Flowers	0.89	0.19	0.92	143	69
Horses	0.83	0.21	0.88	252	74
Mountains	0.50	0.20	0.61	337	80
Food	0.64	0.27	0.73	248	66
Total	٠,٧١	٠,٢٦	٠,٧٨	٢٦٧	١١٩

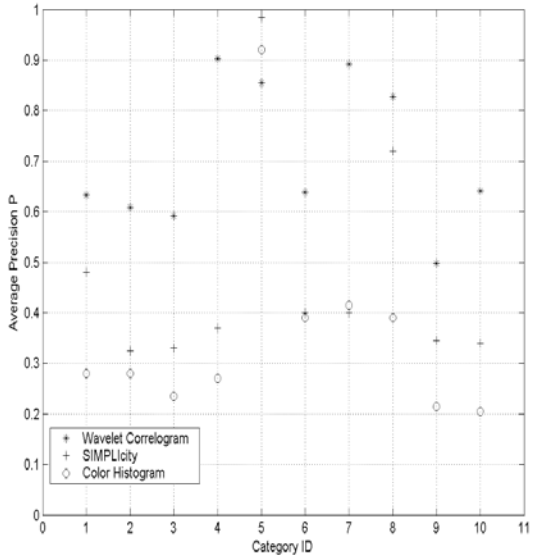
Average Precision P
Category ID
Wavelet Correlogram
SIMPLIcity
Color Histogram

(a)

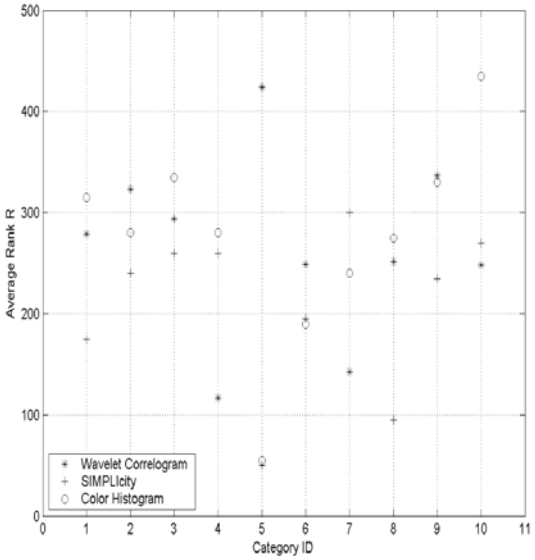
Average Rank R
Category ID
Wavelet Correlogram
SIMPLIcity
Color Histogram

(b)

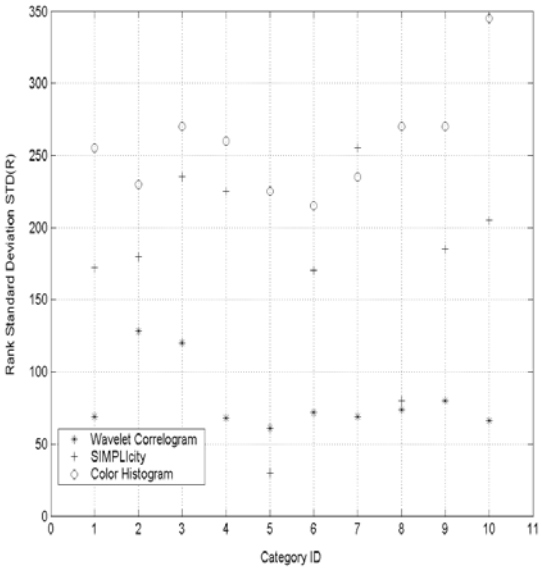
Rank Standard Deviation STD(R)
Category ID
Wavelet Correlogram
SIMPLIcity
Color Histogram

(c)

Method	Image Size	DB Size	Feature Vector Size (bytes)	Computational Cost	Precision (P)	Weighted Precision (WP)
WBIIS	**128x128**	**10000**	**>768**	***O(NlogN)***	**<0.48**	**0.253***
SIMPLIcity	**384x256**	**1000**	***O(M)***	***O(NlogN)***	**0.453****	**0.525***
Color Correlogram	**232x168**	**14554**	***O(MK)***	***$O(N^2K)$***	**0.57**	**NA**
Edge Correlogram	**Different sizes**	**10000**	**288**	***$O(N^2)$***	**0.66*****	**NA**
Wavelet Correlogram	**Different sizes**	**1000**	**384**	***$O(N^2)$***	**0.71**	**0.78**

*** Using the results reported in [14].**
**** Estimated value using the results reported in [5].**
***** With normalization against rotation [15].**